Drug Design, Development and Therapy

Dovepress
open access to scientific and medical research

Open Access Full Text Article

ORIGINAL RESEARCH

Integrated Network Pharmacology Analysis and Experimental Validation to Elucidate the Mechanism of Acteoside in Treating Diabetic Kidney Disease

Shu Jiao Zhang[1,2,*], Yi Fei Zhang[1,2,*], Xue Hui Bai[1,2], Meng Qi Zhou[1,2], Ze Yu Zhang[1,2], Shuai Xing Zhang[1,2], Zi Jing Cao[1,2], Lin Wang[1,2], Shao Wei Ding[1,2], Hui Juan Zheng[1,2], Yu Ning Liu[1–3], Guo Yong Yu[1], Wei Jing Liu[1–3]

[1]Dongzhimen Hospital, Beijing University of Chinese Medicine, Beijing, People's Republic of China; [2]Key Laboratory of Chinese Internal Medicine of Ministry of Education, Beijing Dongzhimen Hospital, Beijing University of Chinese Medicine, Beijing, People's Republic of China; [3]Renal Research Institution of Beijing University of Chinese Medicine, Beijing University of Chinese Medicine, Beijing, People's Republic of China

*These authors contributed equally to this work

Correspondence: Guo Yong Yu, Dongzhimen Hospital, Beijing University of Chinese Medicine, No. 5 Haiyuncang, Beijing, Dongcheng District, 100700, People's Republic of China, Email 18901133535@163.com; Wei Jing Liu, Renal Research Institution of Beijing University of Chinese Medicine, and Key Laboratory of Chinese Internal Medicine of Ministry of Education and Beijing, Dongzhimen Hospital, Beijing University of Chinese Medicine, Beijing, People's Republic of China, Tel/Fax +86-010-84013190, Email 1977@hotmail.com

Background: Acteoside, an active ingredient found in various medicinal herbs, is effective in the treatment of diabetic kidney disease (DKD); however, the intrinsic pharmacological mechanism of action of acteoside in the treatment of DKD remains unclear. This study utilizes a combined approach of network pharmacology and experimental validation to investigate the potential molecular mechanism systematically.

Methods: First, acteoside potential targets and DKD-associated targets were aggregated from public databases. Subsequently, utilizing protein-protein interaction (PPI) networks, alongside GO and KEGG pathway enrichment analyses, we established target-pathway networks to identify core potential therapeutic targets and pathways. Further, molecular docking facilitated the confirmation of interactions between acteoside and central targets. Finally, the conjectured molecular mechanisms of acteoside against DKD were verified through experimentation on unilateral nephrectomy combined with streptozotocin (STZ) rat model. The underlying downstream mechanisms were further investigated.

Results: Network pharmacology identified 129 potential intersected targets of acteoside for DKD treatment, including targets such as AKT1, TNF, Casp3, MMP9, SRC, IGF1, EGFR, HRAS, CASP8, and MAPK8. Enrichment analyses indicated the PI3K-Akt, MAPK, Metabolic, and Relaxin signaling pathways could be involved in this therapeutic context. Molecular docking revealed high-affinity binding of acteoside to PIK3R1, AKT1, and NF-κB1. In vivo studies validated the therapeutic efficacy of acteoside, demonstrating reduced blood glucose levels, improved serum Scr and BUN levels, decreased 24-hour urinary total protein ($P<0.05$), alongside mitigated podocyte injury ($P<0.05$) and ameliorated renal pathological lesions. Furthermore, this finding indicates that acteoside inhibits the expression of pyroptosis markers NLRP3, Caspase-1, IL-1β, and IL-18 through the modulation of the PI3K/AKT/NF-κB pathway.

Conclusion: Acteoside demonstrates renoprotective effects in DKD by regulating the PI3K/AKT/NF-κB signaling pathway and alleviating pyroptosis. This study explores the pharmacological mechanism underlying acteoside's efficacy in DKD treatment, providing a foundation for further basic and clinical research.

Keywords: DKD, acteoside, network pharmacology, experimental verification

Received: 18 October 2023
Accepted: 5 April 2024
Published: 30 April 2024

Introduction

Diabetic Kidney Disease (DKD) is one of the prominent microvascular complications associated with diabetes mellitus. The underlying pathogenesis of DKD involves a complex interplay of factors such as genetic susceptibility, metabolic dysregulation, hemodynamic changes, inflammation, and oxidative stress, among other biochemical mechanisms.[1] Conventional treatment modalities for DKD primarily involve rigorous control of blood glucose and blood pressure, as well as the blockade of the Renin-Angiotensin-Aldosterone System (RAAS). However, these interventions only slow the progression of the disease and fail to either prevent exacerbation or reverse the pathological process.[2,3] Globally, DKD is a significant contributor to end-stage renal disease (ESRD), with approximately 20% to 50% of diabetes mellitus patients eventually developing DKD.[4] This constitutes a critical public health crisis worldwide.[5] Notably, DKD has now overtaken glomerulonephritis as the principal cause of Chronic Kidney Disease (CKD) in China.[6] Consequently, research into the development of safe and efficacious novel therapeutics has moved to the forefront of DKD research. Given their multi-pathway and multi-target action mechanisms, Chinese medicines hold potential in the treatment of DKD,[7] thereby emerging as a pivotal area for new drug exploration.

Acteoside (ACT, also named as Verbascoside), molecular formula $C_{29}H_{36}O_{15}$, named the α-L-rhamnosyl-(1->3)-β-D-glucoside of hydroxytyrosol, belongs to the cinnamate and disaccharide derivatives, which can be classified into phenylethanol glycoside compounds family. ACT is widely found in a variety of botanical medicines in the Oleaceae, Dicotyledons, Verbenaceae and other botanicals, such as Rehmannia glutinosa, Cistanche deserticola, Forsythia suspensa,[8–10] etc. ACT has been proven to have various pharmacological effects such as cardiovascular protection, anti-tumor, anti-infection, anti-hepatotoxicity, anti-neurotoxicity, anti-hyperuricemia, regulation of blood glucose,[11–15] etc. Particularly noteworthy is the protective effect of ACT on renal lesions by reducing oxidative stress, inhibiting inflammatory responses, modulating immune function, improving tissue hemodynamics, and mitigating fibrotic lesions.[16,17] However, the potential mechanism of ACT in the treatment of DKD has not yet been fully clarified, and revealing the intrinsic mechanism of action by which ACT exerts a therapeutic effect on DKD is a meaningful study.

Network pharmacology serves as a comprehensive approach to screen bioactive compounds, predict target proteins and identify signaling pathways from a molecular vantage point. By integrating these elements with disease-specific target genes into biomolecular networks,[18,19] the methodology provides a systemic overview of the interrelation among compounds, protein/gene targets, and diseases. Complementary to this, molecular docking models the interaction between an active drug ingredient and a target protein receptor, offering insights into their binding affinity and mechanisms of action. The primary objective of this study is to employ both network pharmacology and molecular docking techniques to explore the underlying mechanisms by which ACT provides renoprotection against DKD. To further substantiate our findings, we also conducted in vivo validations to confirm the therapeutic efficacy of ACT in treating DKD. The detailed process of the research is displayed in Figure 1.

Materials and Methods

Collection of ACT Chemistry and Prediction of Potential Drug Targets

The 2D structural information of ACT was sourced from the PubChem database (https://pubchem.ncbi.nlm.nih.gov/). To identify the potential targets for ACT's mechanism of action, we employed a diverse array of databases, including the ChEMBL database (https://www.ebi.ac.uk/chembl/), the PharmMapper database (http://www.lilab-ecust.cn/pharmmapper/), the Swiss Target Prediction database (http://swisstargetprediction.ch/), the Super-PRED database (https://prediction.charite.de/), and the TCMSP database (http://tcmspw.com/tcmsp.php). In each database, the species parameter was set to "Homo sapiens" to focus on human-relevant targets. Subsequently, the protein information for ACT was normalized using the UniProt database (https://www.uniprot.org/).

Prediction of DKD Disease Targets

To identify disease-specific targets for DKD, we employed the keywords "Diabetic Kidney Disease" and "Diabetic Nephropathy" for our search across multiple databases. These databases included GeneCards (https://www.genecards.org/), DisGeNET (https://www.disgenet.org/), OMIM (https://www.omim.org/), DrugBank (https://go.drugbank.com/),

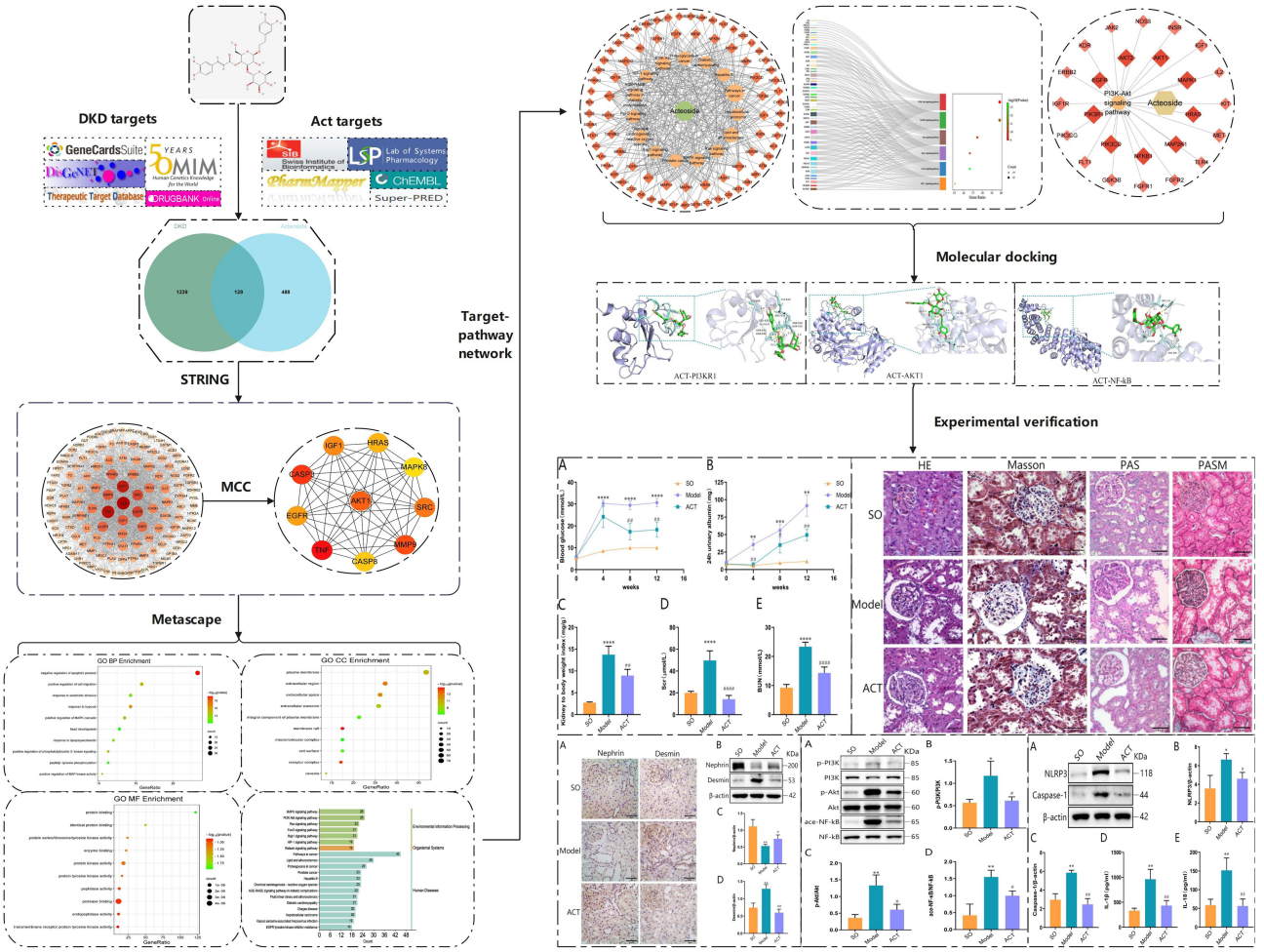

Figure 1 Flow chart of present research.

and the Therapeutic Target Database (https://db.idrblab.net/ttd/). Subsequently, the target data were normalized using the UniProt database. The extracted targets from these public databases were consolidated and duplicate entries were eliminated to yield a refined list of DKD-relevant targets. Utilizing the Bioinformatics Mapping Tool (http://www.bioinformatics.com.cn/), we identify common targets between the drug and the disease, which were subsequently visualized using a Venn diagram.

Constructing Protein-Protein Interaction (PPI) Networks

The intersecting targets between ACT and DKD were imported into the String database (https://cn.string-db.org/) for further analysis. The species was specified as "Homo sapiens", and the minimum required interaction score was set to "medium confidence=0.4." Unconnected protein nodes were excluded from the analysis, while all other parameters were retained at their default settings. This approach yielded the PPI relationships among the targets. The resulting data were then exported and visualized using Cytoscape 3.8.0 software to construct the PPI network diagram. Within Cytoscape, we employed the "Cytohubba" plug-in to identify key targets. Utilizing Maximal Clique Centrality (MCC) for topological analysis, we pinpointed the top ten critical genes within the interaction network.

GO and KEGG Functional Enrichment Analysis

We imported the intersecting proteins between ACT and DKD into the DAVID database (https://david.ncifcrf.gov/), where we conducted an in-depth analysis of their biological processes and metabolic pathways. This analysis was carried out using gene ontology (GO) for biological process (BP), cellular composition (CC), and molecular function (MF), as

well as the Kyoto Encyclopedia of Genes and Genomes (KEGG) for pathway analysis. Subsequently, the top 25 KEGG pathways and the top 10 GO enrichment results were visualized using the Bioinformatics Mapping Tool.

Constructing a "Component-Pathway-Target" Network

Based on the enrichment analysis results, we selected the top 15 KEGG signaling pathways and their target information. We then matched ACT with the targets enriched on these pathways. After importing the matched data into Cytoscape, we constructed a target-pathway network for ACT in the treatment of DKD and identified key pathways and core target proteins.

Molecular Docking

Molecular docking simulates the complementary shapes and properties of ligand-receptor interactions, allowing for further exploration of the interactions between ACT and potential action targets at the molecular level. Initially, the 2D structure of ACT was sourced from the PubChem database in SDF format and then converted to a 3D format using OpenBabel. This was followed by preprocessing steps that included adding hydrogen bonds and setting torsional bonds, executed through AutoDockTools software. Subsequently, we selected core targets from the previously identified key pathways and handpicked the corresponding 3D protein structures from the PDB database. Utilizing PyMOL and AutoDockTools, we performed additional steps like removing water molecules and adding hydrogen bonds. The preprocessed ACT and target protein structures were then imported into AutoDockTools for semi-flexible docking. The results with the lowest binding energy were selected, and the corresponding docking models were visualized using PyMOL software.

Animal Model Construction and ACT Intervention

A total of 30 male SPF Sprague-Dawley rats, aged between 6 to 8 weeks and weighing approximately 200±20g, were acquired from Beijing Weitong Lihua Experimental Animal Technology Co., Ltd. (Beijing, China). These rats were housed under controlled conditions at the SPF Animal Laboratory of the Beijing University of Chinese Medicine. The housing environment was maintained at a temperature range of 23–26°C and a relative humidity of 40–60%, with a 12-hour light-dark cycle. Rats had ad libitum access to water and were fed standard rodent chow. Ethical approval for the study was granted by the Animal Ethics Committee of Beijing University of Chinese Medicine (Approval number: BUCM-4-2,020,120,501-4182) and was performed in conformity to the Guide for the Care and Use of Laboratory Animals. Following a one-week acclimation period, the 30 rats were randomly allocated into two groups: the sham-operation group (SO; n=10) and the surgical operation group (n=20). Before the surgical procedures, all rats underwent a 12-hour fasting period. Anesthesia was then administered through intraperitoneal injection of 1% pentobarbital sodium at a dosage of 50mg/kg. The rats were positioned in right lateral recumbency, and a 1.5 cm longitudinal incision was made 1–2cm below the lower edge of the left rib and 1cm lateral to the vertebral midline. The skin and muscle layers were dissected to expose the left kidney. In the surgical operation group, the renal capsule was carefully excised, the renal pedicle ligated, and the left kidney removed. Subsequently, layered suturing of the abdominal wall was performed. Conversely, in the sham-operation group, only the left kidney was exposed, followed by immediate closure of the abdominal incision. Before suturing, any intraperitoneal effusion was absorbed using sterile cotton balls, and a suitable quantity of cephalosporin powder was applied to all surgical wounds. Two weeks following the surgical procedures, all rats underwent a 12-hour fasting period without water deprivation. Rats in the operation group were given a single intraperitoneal injection of 50 mg/kg STZ (S0130-1G, Sigma-Aldrich, Shanghai, China), prepared by dissolving STZ powder in a 0.1 M sodium citrate buffer (pH 4.5) to yield a 1% STZ solution immediately before use. In contrast, rats in the sham operation (SO) group received an intraperitoneal injection of an equivalent volume of sodium citrate buffer. Blood glucose levels were assessed two hours post-injection. Consistent blood glucose readings exceeding 16.7 mmol/L for three consecutive days, including the day of the measurement, served as an indicator of successful model establishment. Upon successful establishment of the animal model, the rats were stratified into two groups (the Model group and the ACT group) utilizing a random number table methodology. Gavage treatment commenced on the third day post-modeling. Rats in the ACT group were administered ACT (HB0067, Jiangsu Yongjian Pharmaceutical Technology Co.,

Ltd, Jiangsu, China) at a dosage of 50 mg/kg/day via oral gavage,[16] once daily, for a continuous duration of 12 weeks. Concurrently, rats in both the Model group and the SO group received an equivalent volume of normal saline via oral gavage for the same 12-week period.

Measurement of the Kidney to Body Weight Ratio

Kidney-to-body weight ratio serves as a quantitative indicator of renal hypertrophy and can also provide an indirect assessment of the extent of renal fibrosis. Following anesthesia, the rats were weighed to determine their body mass. Subsequently, the right kidneys were excised, rinsed in 4°C saline solution, and then blotted dry using filter paper to remove any surface moisture. The mass of the right kidney was then weighed, and the renal index was calculated using the formula: Renal Index = (kidney mass (g) / rat body mass (g))× 100%.

Measurement of Biochemical Indicators

Blood samples were periodically collected from the tail tip at four-week intervals, both before and after the establishment of the animal model, for the assessment of random blood glucose levels. Following this, the rats were subjected to fasting and then housed in metabolic cages for the collection of 24-hour urine samples. The volume of urine was recorded, and the samples were subsequently subjected to centrifugation at 4°C and 3000 rpm for 10 minutes. The supernatant was aliquoted and stored at −80°C for subsequent analyses. Urinary protein concentrations were quantified using a specialized urinary protein assay kit (Nanjing, Jiancheng Bioengineering Institute, Nanjing, China). After the 12-week treatment regimen, the rats were fasted for 12 hours before arterial blood collection via the abdominal aorta. The collected samples were stood for 30 minutes at room temperature before being centrifuged at 4°C and 3500 rpm for 15 minutes. The serum was then aliquoted and stored at −80°C for future analyses. Serum urea nitrogen (BUN) levels and serum creatinine (Scr) concentrations were quantified with an assay kit (Nanjing, Jiancheng Bioengineering Institute, Nanjing, China).

Pathological Examination of Renal Tissue

Rat kidney tissues were fixed in 4% paraformaldehyde for 48 hours, followed by a sequential process of dehydration through an ethanol gradient, clearance in xylene, immersion in wax, and embedding in paraffin, to prepare sections with a thickness of 3μm. After deparaffinization and rehydration, the tissue sections were stained according to the instructions provided in the staining kit using Hematoxylin and Eosin (H&E), Masson's Trichrome, Periodic Acid-Schiff (PAS), and Periodic Acid-Silver Methenamine (PASM) stains. Pathological alterations in the renal tissues were examined under a light microscope, and representative images were captured for further analysis.

Immunohistochemistry on Renal Tissue

Following deparaffinization, antigen retrieval, and inhibition of endogenous peroxidase activity, the 3 μm-thick paraffin-embedded kidney tissue sections were incubated with primary antibodies against Desmin (1:2000, ab32362, Abcam, UK) and Nephrin (1:1000, ab216341, Abcam, UK), at 4°C overnight. This was followed by incubation with the appropriate secondary antibodies. Subsequently, the sections were incubated with the secondary antibody. Visualization was facilitated through DAB chromogenic staining followed by counterstaining with hematoxylin, differentiation, a graded ethanol dehydration series, and xylene clearance. Observations and image acquisitions were executed under a 400× optical microscope.

Western Blot Analysis

Rat kidney tissue samples were mechanically disrupted and lysed using RIPA lysis buffer (Applygen, Beijing, China) to facilitate protein extraction. Following centrifugation, the supernatant containing the proteins was harvested. The protein concentration was subsequently determined through a BCA protein assay, followed by heat denaturation in the presence of a loading buffer. Equal volumes of the protein samples (10 μL per well) were loaded onto an SDS-PAGE gel for electrophoretic separation. After the separation process, the proteins were transferred onto a nitrocellulose (NC) membrane utilizing the wet transfer method. The membrane was then blocked with 5% skim milk and subsequently incubated overnight at 4°C with primary antibodies, including PI3K (1:1000, #4292, CST, Boston, USA), p-PI3K

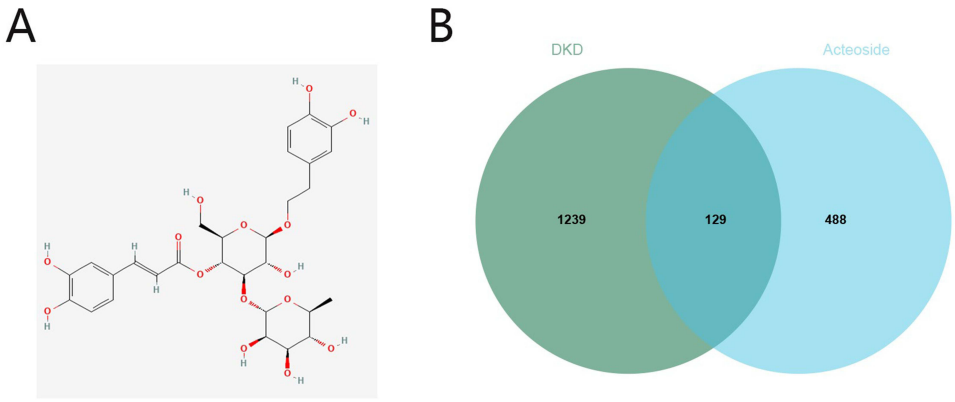

Figure 2 (**A**) The chemical structure of ACT. (**B**) Venn diagram of the overlapping genes of ACT and DKD.

(1:1000, AF3242, Affinity Biosciences, Liyang, China), AKT (1:1000, #4691, CST, Boston, USA), p-AKT (1:1000, #9271, CST, Boston, USA), NF-κB (1:2000, ab16502, Abcam, UK), acetylated NF-κB (1:1000, #12629, CST, Boston, USA), NLRP3 (1:1000, ab270449, Abcam, UK), Caspase-1 (1:2000, ab286125, Abcam, UK), and β-actin (1:2000, ab8226, Abcam, UK). Post incubation, the membrane was washed with TBST to remove unbound antibodies, before incubation with HRP-conjugated secondary antibodies (either anti-rabbit or anti-mouse IgG) for 1 hour. The membrane was then developed using an ECL kit (P1010, Biosharp, Beijing, China), and the resulting bands were analyzed quantitatively using ImageJ software for densitometry analysis.

ELISA Assay

IL-1β and IL-18 levels in rat kidney tissues were quantified using ELISA kits (IL-1β: E-EL-R0012c; IL-18: E-EL-R0567c, Elabscience, Wuhan, China). Tissues were collected, weighed, minced, and lysed with RIPA buffer containing protease and phosphatase inhibitors. After homogenization, the lysates were centrifuged at 10,000 rpm for 15 minutes at 4°C to obtain the protein supernatants. The protein concentrations were then determined using a BCA Protein Assay Kit. Samples were then processed as per the ELISA kit instructions and analyzed with a microplate reader to determine IL-1β and IL-18 protein levels.

Statistical Analysis

All statistical analyses were performed utilizing SPSS 20.0 software (IBM, Chicago, IL, USA). Data are presented as mean ± SD. To ensure reliability, each independent experiment was conducted a minimum of three times. Comparative analyses between two groups were executed using Student's *t*-test, whereas one-way ANOVA was employed for comparisons involving multiple groups. p-value<0.05 was considered to indicate statistical significance.

Results

Prediction of ACT Potential Targets of Action and DKD-Related Targets

The molecular structure of ACT is depicted in Figure 2A and physicochemical characteristics were summarized in Table 1. Utilizing multiple databases, including CHEMBL, PharmMapper, Swiss Target Prediction, Super-PRED, and TCMSP, and removing duplicate entries, we identified 617 potential targets for ACT. Subsequent analysis utilizing

Table 1 Chemical Information of the Active Compounds of Acteoside

Name	CAS	MW	AlogP	Hdon	Hacc	LogKp	BA	SA	TPSA	MR
Acteoside	61,276–17-3	624.59	−0.43	9	15	−10.46	0.17	6.37	245.29	148.42

Abbreviations: MW, molecular weights; AlogP, Algorithm LogP; Hdon, hydrogen bond donor; Hacc, hydrogen bond acceptor; Log Kp, Log skin permeation; BA, Bioavailability Score; SA, Synthetic accessibility; TPSA, topological polar surface area; MR, Molar Refractivity.

resources such as the GeneCards, DisGeNET, OMIM, DrugBank, and the Therapeutic Target Database facilitated the isolation of 1368 distinct targets associated with DKD disease, following the elimination of duplicates. A Venn diagram analysis of the 1368 DKD disease-related targets and the 617 ACT-associated targets revealed a subset of 129 common targets (Figure 2B).

PPI Network Analysis

To elucidate the relationship between ACT and DKD targets and to pinpoint central therapeutic nodes, we performed a PPI analysis on the 129 shared targets using the STRING database, visualized through Cytoscape. This yielded a network graph encompassing 1699 edges and 129 nodes (Figure 3A). Subsequent analysis via CytoHubba topology revealed the top ten critical targets, including AKT1, TNF, Casp3, MMP9, SRC, IGF1, EGFR, HRAS, CASP8, and MAPK8 (Figure 3B). These proteins represent key targets of ACT for DKD, holding potential significance for subsequent molecular docking and signaling pathway identification.

Enrichment Analysis

To elucidate the therapeutic effects and underlying molecular mechanisms of the drug component targets at the gene function level, we conducted an enrichment analysis of the 129 intersection targets utilizing the DAVID database. The analysis identified 635 biological processes (BP), 140 molecular functions (MF), and 73 cellular components (CC) implicated in ACT's therapeutic role in DKD treatment. The analysis highlighted primary BPs such as the negative regulation of apoptotic processes, response to hypoxia, and the facilitation of phosphatidylinositol 3-kinase signaling. Key MFs involve activities including protein binding, identical protein binding, and kinase activity associated with serine, threonine, and tyrosine. The CC analysis pinpointed associations with structures such as the plasma membrane, extracellular regions, and membrane rafts. Following a comprehensive analysis, the top 10 functional characteristics were visualized (Figure 4A-C). Subsequently, KEGG pathway analysis discerned 156 signaling pathways, and the top 20 pathways were visualized according to the number of enriched targets. The results included the PI3K-Akt signaling pathway, MAPK signaling pathway, Pathways in cancer, Metabolic pathways, Relaxin signaling pathway, etc. (Figure 4D). The findings above lay a foundation for understanding the potential therapeutic mechanisms of ACT in DKD.

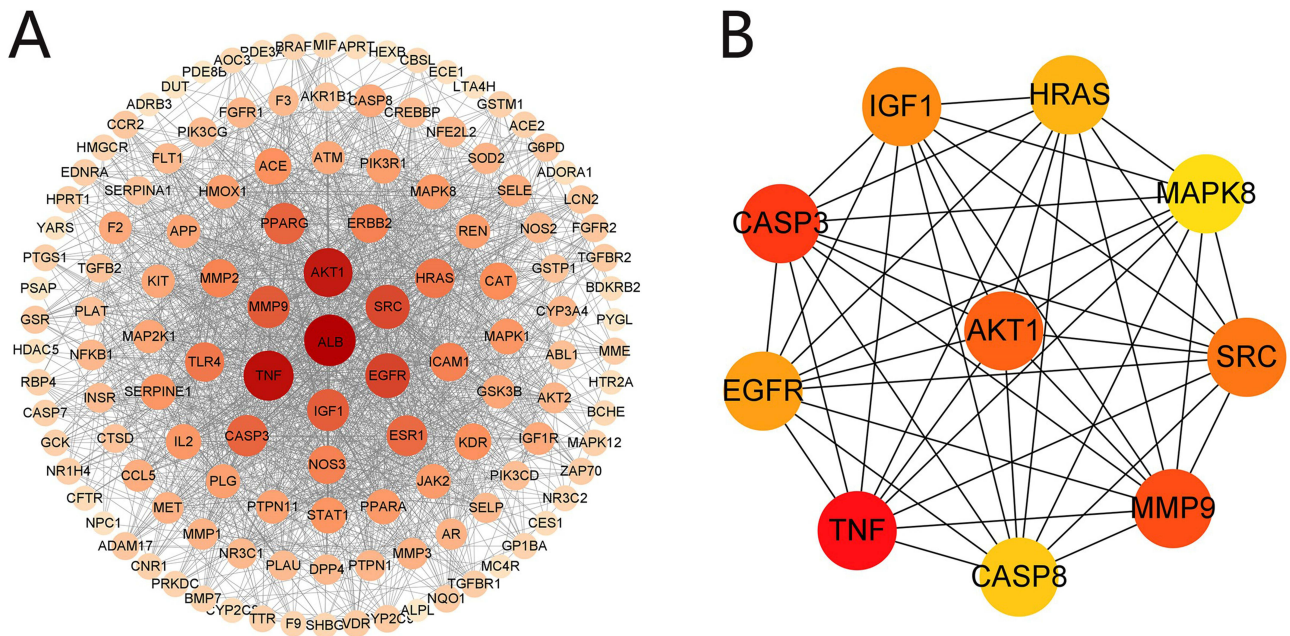

Figure 3 PPI network for ACT in treatment of DKD. (**A**) PPI network (129 nodes and 1699 edges) of the ACT ingredient targets against DKD, which was produced using STRING. The node size and color depth are proportional to the degree values. (**B**) The high-relevant targets' intersection of DKD and ACT. The top 10 targets were screened according to their MCC score, including AKT1, TNF, CASP3, MMP9, SRC, IGF1, EGFR, HRAS, CASP8 and MAPK8.

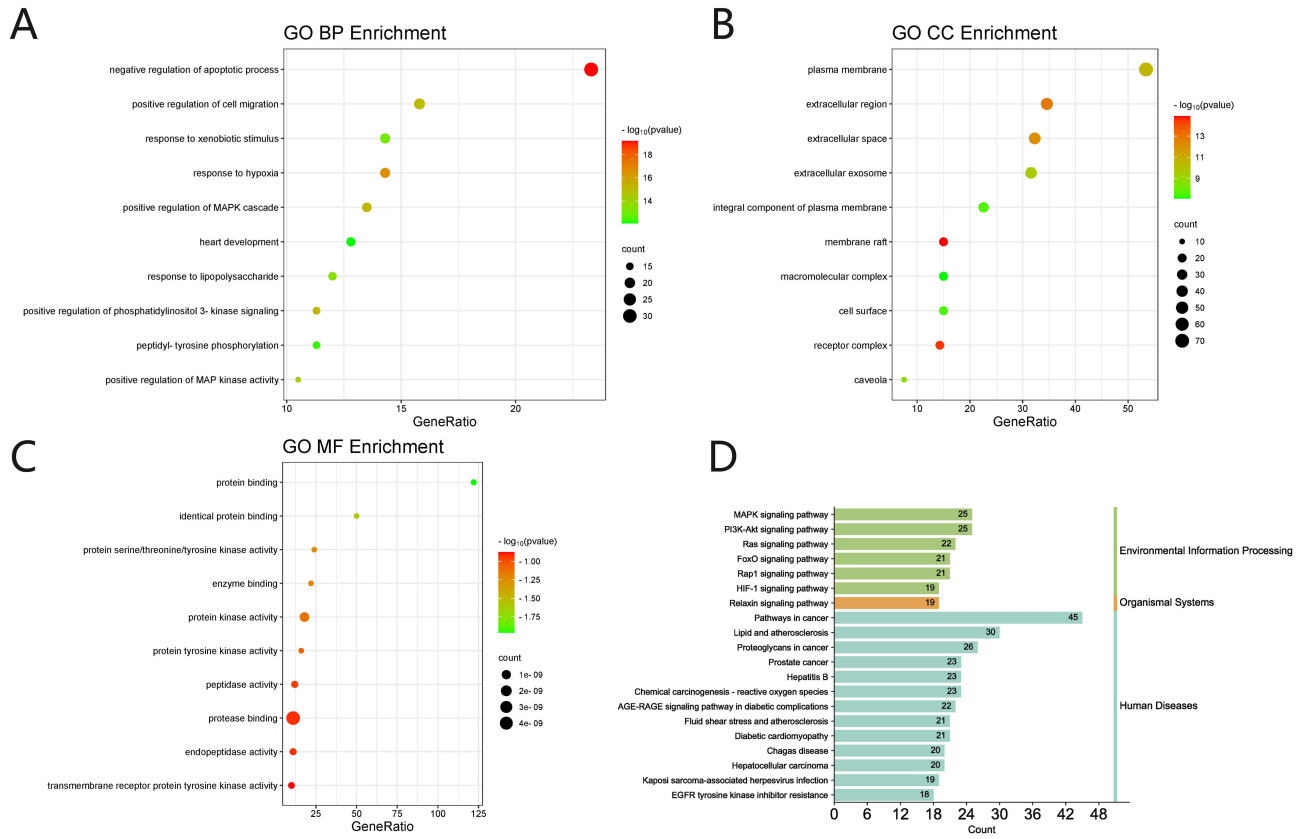

Figure 4 GO and KEGG pathway enrichment analysis of ACT in treatment of DKD. (**A-C**) GO enrichment analysis of the key targets. The numbers on the X-axis indicate the number of target genes in the enrichment analysis, the bubble size and the red blood cell size. The numbers on the X-axis indicate the number of target genes in the enrichment analysis, the bubble size and the red depth indicate its significance. (**D**) KEGG pathway analysis of intersection targets. indicates the number of genes annotated to this pathway. Different colors indicate different KEGG pathway classifications.
Abbreviations: BP, biological processes; CC, cell component; MF, molecular function.

"Component-Pathway-Target" Network

To elucidate the potential mechanisms underlying ACT's efficacy in treating DKD, we constructed a target gene pathway network centered around the 15 principal pathways and 78 corresponding target genes (Figure 5A). This network suggests that ACT may exert synergistic therapeutic effects on DKD through various signaling pathways. Further screening the Environmental Information Processing from the key pathways and visualizing the data through a Sankey diagram (Figure 5B), in conjunction with the PPI network, enrichment, and "component-pathway-target" analysis results, highlighted the PI3K/AKT pathway is the core pathway in ACT's therapeutic strategy against DKD. Furthermore, we delineated the ACT and PI3K/AKT pathway subnetwork, facilitating the identification of the key ACT targets in DKD treatment via the PI3K/AKT signaling pathway (Figure 5C).

Molecular Docking

To elucidate the interaction dynamics between ACT and PI3K/AKT pathway-associated genes, molecular docking simulations were employed. The core proteins of this pathway, namely AKT1, PI3KR1 and NF-κB1, were individually docked with ACT, and their respective binding energies were calculated. Lower binding energy values indicate higher stability of ACT interaction with the core targets. Acteoside and three specific targets were respectively selected as small molecule ligands and protein receptors (Table 2). ACT bound with PI3KR1 (PDB ID: 5AUL) via hydrogen bonds formed with amino acid residues GLY-640, ASN-636, ASN-632, GLU-635, and GLY-665; exhibiting a binding energy of −6.16 kcal/mol (Figure 6A). ACT interacted with AKT1 (PDB ID: 7NH5) via hydrogen bonds with residues PHE-368, ILE-366, LYS-386, LYS-385, SER-381, and LYS-177; exhibiting a binding energy of −4.96 kcal/mol (Figure 6B). ACT formed bonds with NF-κB1 (PDB ID: 7LFC) via interactions with amino acid residues SER-144 and ARG-438;

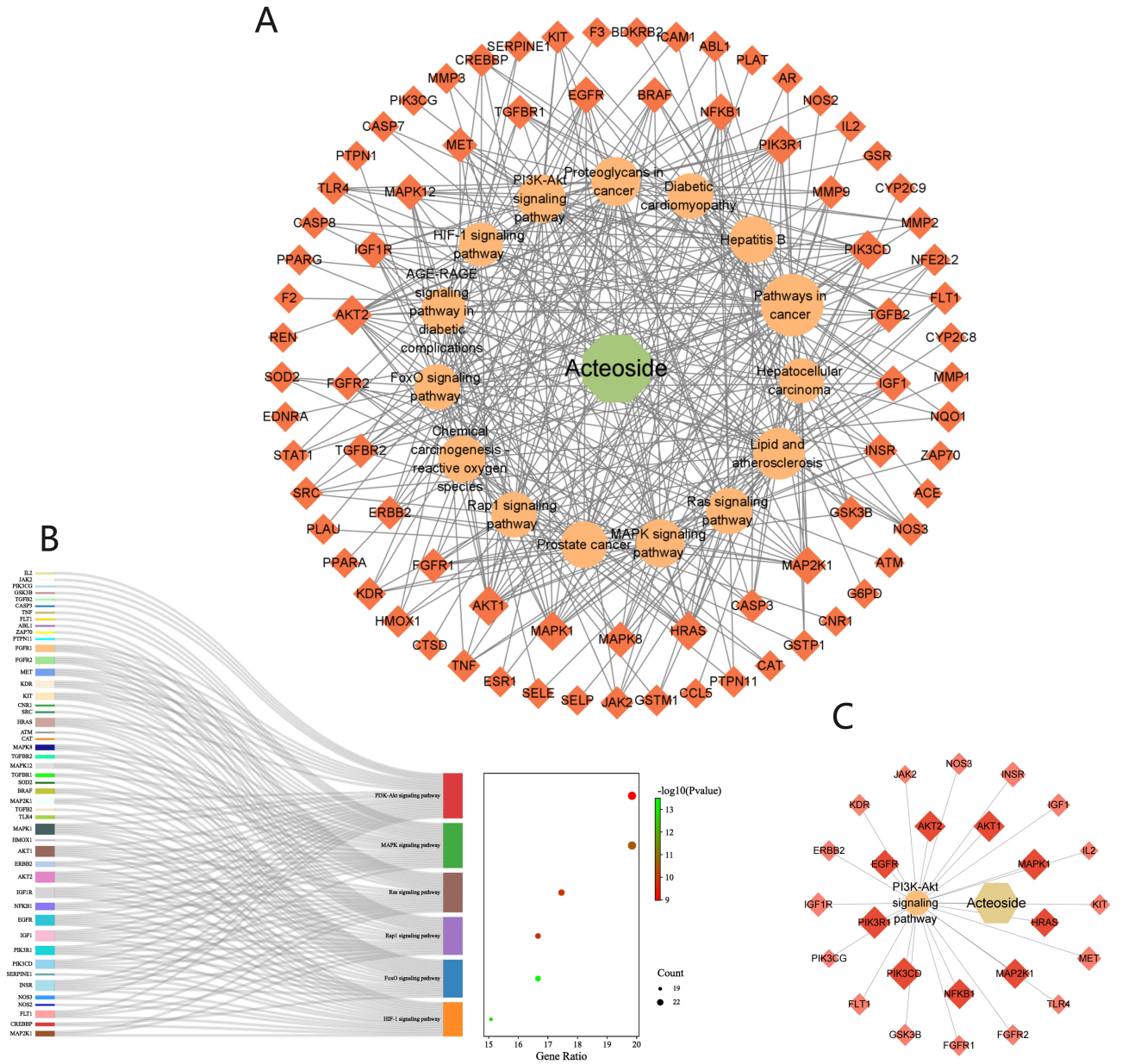

Figure 5 "Target-Pathway" Network of ACT against DKD. (**A**) The nodes in the network display targets. represents the signaling pathway of ACT in the treatment of DKD and the diamond node represents the corresponding target. (**B**) The numbers on the X-axis indicate the number of target genes in the enrichment analysis, the bubble size and the number of target genes in the enrichment analysis. indicate the number of target genes in the enrichment analysis, the bubble size and the red depth indicates its significance. (**C**) The deep red diamond indicates the key targets of ACT in the treatment of DKD. indicates the key targets of ACT in the treatment of DKD through the PI3K / AKT signaling pathway.

exhibiting a binding energy of −1.54 kcal/mol (Figure 6C). According to established criteria, binding energies<-1.2kcal/mol or −5kJ/mol indicate effective binding. Therefore, all the observed interactions exhibited satisfactory binding, in line with initial predictions.

ACT Improves Physical and Biochemical Indicators in the Rat Model of DKD

In this research, we employed a unilateral nephrectomy alongside STZ injection to establish a rat model of diabetic nephropathy. Post-modeling, blood glucose levels in both the Model and ACT groups exceeded 16.7 mmol/L, a significant increase compared to the SO group, confirming the success of the modeling. Over a 12-week ACT intervention period, the ACT group exhibited a significant decrease in blood glucose levels, most notably at weeks 8

Table 2 Virtual Molecular Docking of Acteoside and Its Targets

No	Compound Name	Target name	Binding energy
1	Acteoside	PIK3R1	−6.16
2	Acteoside	AKT1	−4.96
3	Acteoside	NF-κB1	−1.54

and 12 (Figure 7A), demonstrating ACT's hypoglycemic effect in DKD rats. Subsequently, we quantified vital clinical indicators of renal function, including BUN, Scr, and 24hUTP. The data revealed a significant decrease in 24hUTP in the ACT group in comparison to the Model group, especially at week 4 (Figure 7B). Compared with the Model group, ACT significantly decreased the kidney-to-body weight ratio (Figure 7C) and significantly suppressed the increase of BUN and Scr levels (Figure 7D and E). Collectively, our findings suggest that ACT potentially enhances renal function and improves critical biochemical markers in diabetic nephropathy rats.

ACT Attenuated Renal Histological Damage in the DKD Rats

To meticulously elucidate the renoprotective effect of ACT on DKD rats, renal pathological tissues from each experimental group were harvested and subjected to histological analyses by an optical microscope. HE staining revealed significant pathological changes in the Model group compared to the SO group, including glomerular hypertrophy, enlarged Bowman's capsule space, and renal tubular dilation, along with vacuolar degeneration, swelling, or desquamation of renal tubular epithelial cells. Masson's trichrome staining revealed intact glomeruli, renal tubules, and interstitium in the SO group, with only weak blue staining observed. In contrast, the Model group demonstrated a substantial increase in blue-stained areas within the kidney tissue, indicating an increased degree of fibrosis. PAS and PASM staining revealed that compared with the SO group, the mesangial region in the Model group was significantly widened, the mesangial matrix was proliferated and the Glomerular basement membrane was thickened. Overall, The intervention of ACT significantly improved various renal pathological lesions of the above-mentioned DKD rats (Figure 8).

ACT Reduced Podocyte Injury in DKD Rats

Nephrin, a specific transmembrane protein localized to the slit diaphragm (SD) of podocytes, is pivotal in maintaining SD integrity, while Desmin is expressed only in glomeruli with podocyte damage. Both of them serve as important markers for detecting glomerular injury. Through immunohistochemical staining and Western blotting results, we observed a markedly reduced Nephrin expression in the Model group compared to the SO group, a trend that was reversed following ACT intervention. Interestingly, Desmin expression exhibited a trend inverse to that of Nephrin (Figure 9).

Regulation of the PI3K/AKT Signaling Pathway by ACT

To elucidate the molecular mechanism underlying ACT's therapeutic effect on DKD, we scrutinized the PI3K/AKT signaling pathway based on preceding predictive analyses. We assessed the protein expression levels of PI3K, Akt, and NF-κB by Western blotting (Figure 10A). The results revealed that the expression of phosphorylated PI3K, AKT and acetylated NF-κB was significantly upregulated in the Model group compared with the SO group. After treatment with ACT, their expression was markedly downregulated compared with the Model group (Figure 10 B-D).

Regulation of the PI3K/AKT/NF-kB Downstream Mechanism by ACT

To elucidate the downstream mechanisms of ACT in regulating the PI3K/AKT/NF-kB signaling pathway for DKD treatment, we measured the protein expressions of NLRP3 and Caspase1 using Western blotting (Figure 11A) and quantified IL-1β and IL-18 levels via ELISA. Compared to the SO group, the Model group exhibited significantly elevated levels of NLRP3, Caspase1, IL-1β, and IL-18. After ACT intervention, these levels were notably reduced compared to the Model group (Figure 11B-E).

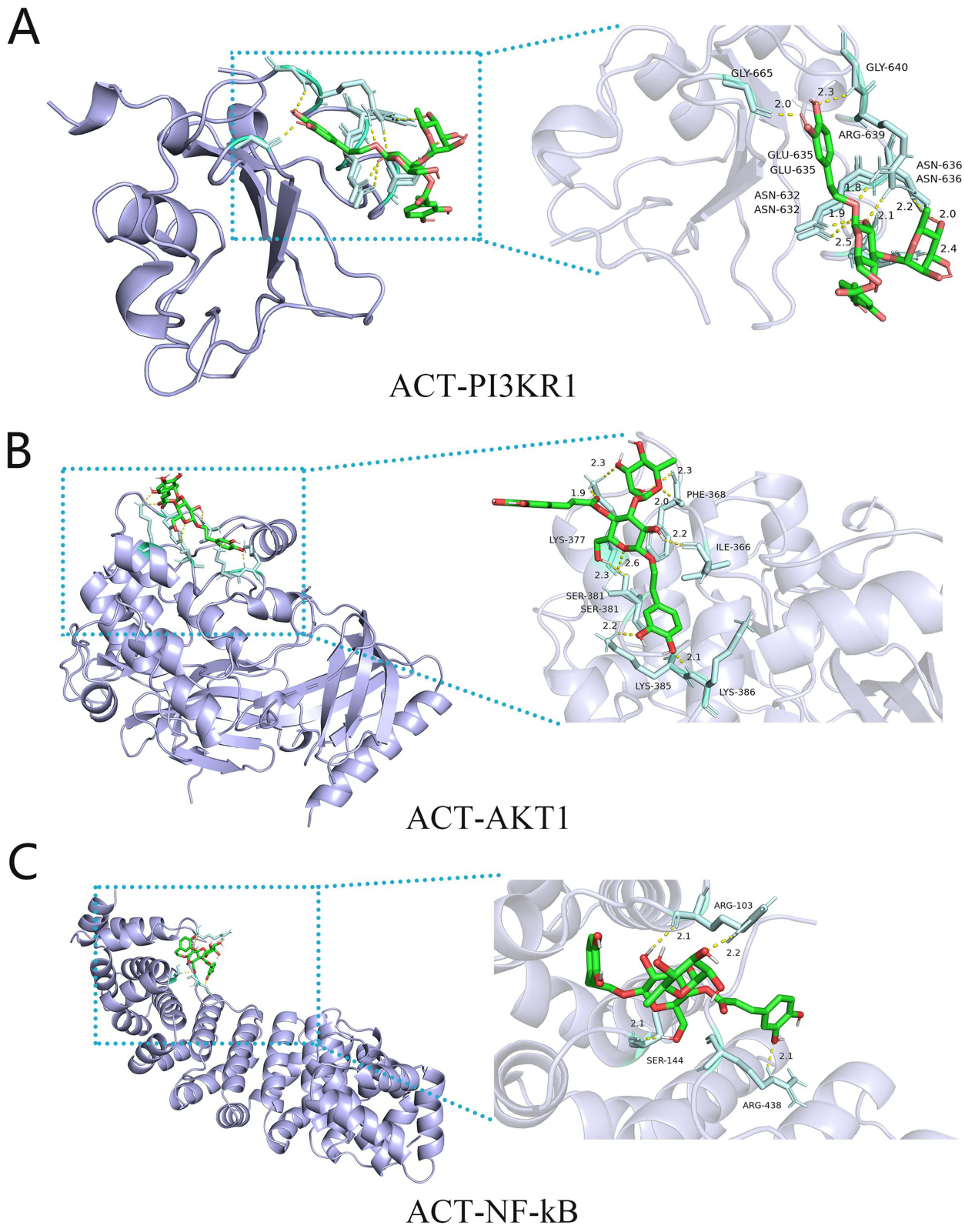

Figure 6 Molecular docking of ACT with PI3KR1 (**A**), AKT1 (**B**), and NF-κB (**C**) shown as 3D diagrams. The number indicates the length of the hydrogen bond.

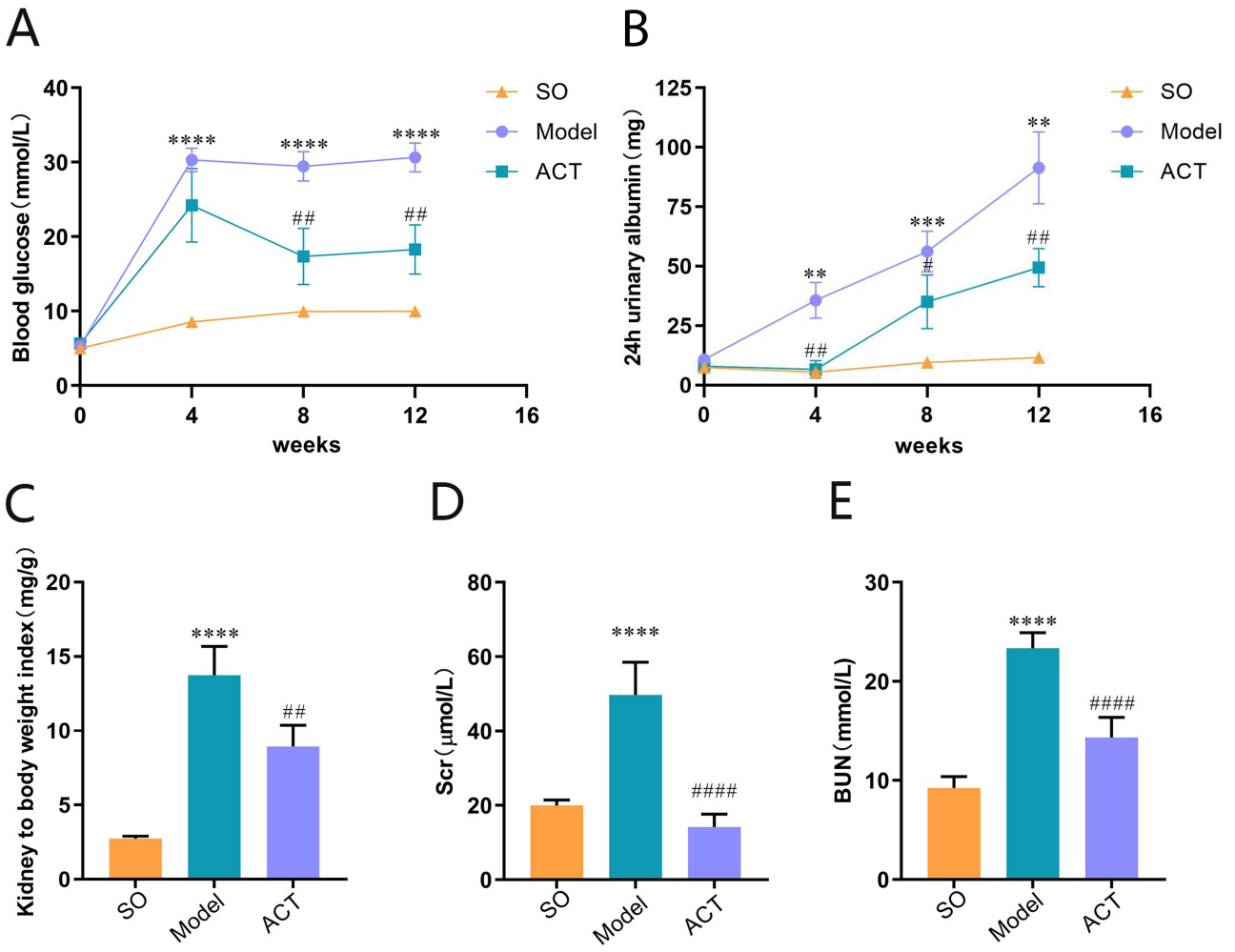

Figure 7 ACT improves physical and biochemical indicators in the rat model of DKD. (**A**) Blood glucose levels. (**B**) 24-h-urine protein levels. (**C**) Kidney to body weight index. (**D**) Scr levels. (**E**) Blood urea nitrogen levels. Data are expressed as mean ± SD, n = 5. **P<0.01, ***P<0.001 and ****P<0.0001 vs sham-operated (SO) group; #P<0.05, ##P<0.01 and ####P<0.0001 vs model (Model) group.

Discussion

Chronic hyperglycemia in diabetes induces all types of cellular dysfunction in the kidney. Diabetic nephropathy can trigger a series of pathological changes, including glomerular basement membrane thickening, extracellular matrix deposition, tubular atrophy, renal interstitial fibrosis and glomerulosclerosis. The natural course of diabetic nephropathy is delineated by phases of glomerular hyperfiltration, progressive proteinuria, and decline in glomerular filtration rate, and eventually culminating in the progression to ESRD. Improving renal function, reducing urinary protein and alleviating pathological changes are important therapeutic strategies for the treatment of DKD.

The therapeutic application of ACT can delay the progression of DKD via its anti-oxidative stress, anti-inflammatory, anti-fibrotic properties and its ability to regulate metabolism.[17,20,21] We used network pharmacology and in vivo validation studies to systematically elucidate the renoprotective mechanisms of ACT on DKD. Our analysis encompassed 617 drug targets associated with ACT and 1369 disease-specific targets of DKD, isolating a total of 129 overlapping targets. Further analysis utilizing Cytohubba's MCC score within the PPI results pinpointed the top ten key targets for ACT therapy in DKD, including AKT1, TNF, Casp3, MMP9, SRC, IGF1, EGFR, HRAS, CASP8, and MAPK8. Meanwhile, GO enrichment analysis and KEGG signaling pathway evaluation of the 129 intersecting targets revealed that the therapeutic effect of ACT on DKD was highly related to 15 signaling pathways, including PI3K/AKT, MAPK,

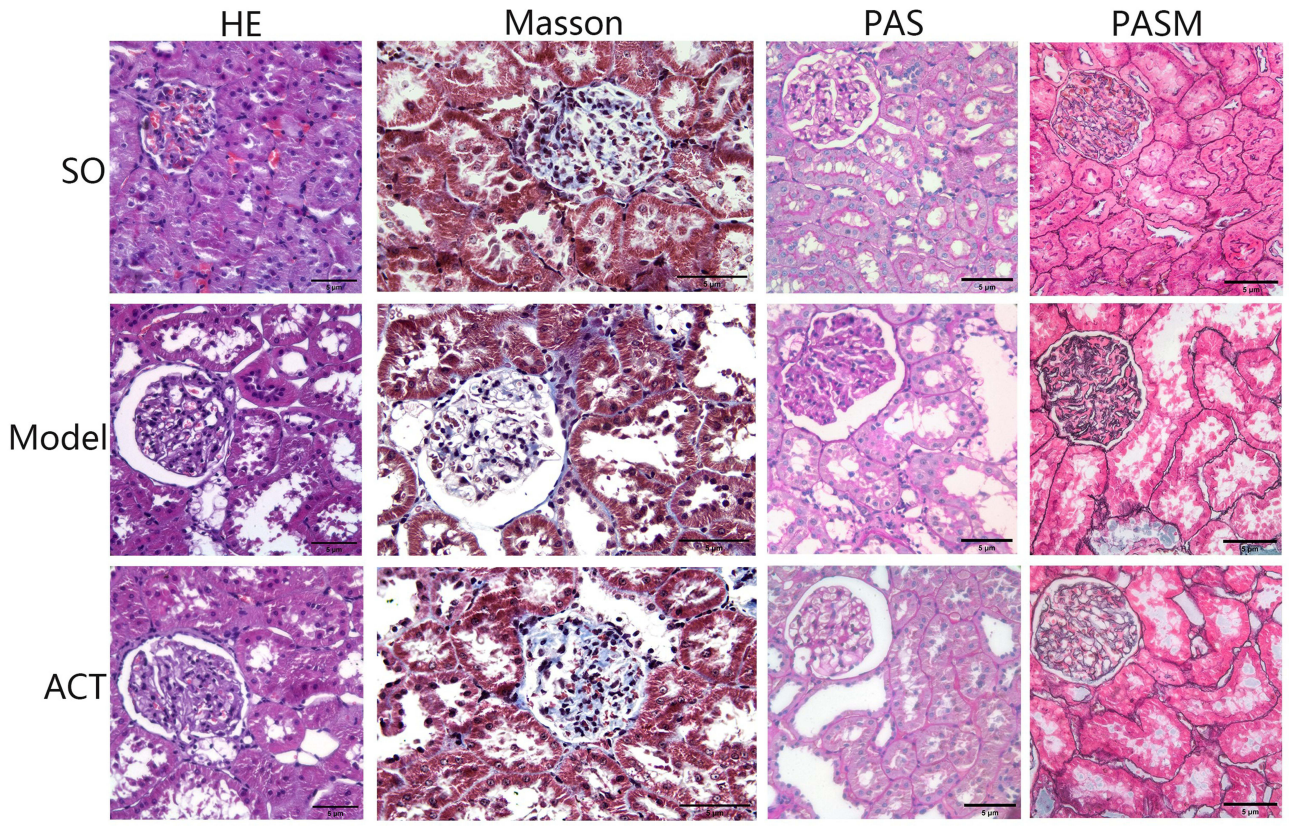

Figure 8 ACT attenuated renal histological damage in the DKD rats. Microstructural images of representative renal tissues stained by HE, Masson, PAS and PASM (400× magnification) (scale bar = 50μm).

RAS, and FOXO. Therefore, we successfully established a DKD model in rats to investigate the therapeutic effect of ACT on DKD and confirm its underlying mechanisms.

In DKD rats treated with ACT, we observed a significant decrease in both SCR and BUN levels. Persistent proteinuria DKD primarily stems from damage to the glomerular filtration barrier (GFB),[22] with the podocyte as a crucial role in its integrity. The protrusions of podocyte cell bodies are referred to as foot processes (FPs), which, through bridging fissures, form the slit diaphragm (SD). The actin cytoskeleton of FPs is connected with SD and glomerular basement membrane (GBM) to maintain the normal structure of podocytes. A critical feature of progressive proteinuria glomerulopathy is podocyte injury, a condition evidenced by the reorganization of the cytoskeleton and marked by increased expression of Desmin protein, an intermediate filament protein of the cytoskeleton, the presence of which correlates positively with the extent of podocyte damage. Additionally, the Nephrin protein forms the transmembrane component of the SD and regulates the cytoskeleton, serving as a critical marker in evaluating podocyte integrity. A critical feature of progressive proteinuria glomerulopathy is podocyte injury, a condition evidenced by the reorganization of the cytoskeleton and marked by increased expression of Desmin protein, an intermediate filament protein of the cytoskeleton, the presence of which correlates positively with the extent of podocyte damage. Additionally, the Nephrin protein forms the transmembrane component of the SD and regulates the cytoskeleton, serving as a critical marker in evaluating podocyte integrity. Our findings demonstrate that ACT intervention significantly reduced 24-UTP levels in rats, accompanied by a decrease in Desmin protein expression and an upregulation of Nephrin protein expression. This suggests that ACT can ameliorate DKD-induced podocyte damage, thereby exerting a protective effect on podocytes.

Subsequently, we extracted a subnetwork delineating the interactions between ACT and the PI3K/AKT pathway from the PPI network, identifying key targets in the PI3K/AKT upstream and downstream pathways including AKT1, AKT2, PIK3R1, PIK3CD, NFκB1, MAPK1, MAP2K1, HRAS, and EGFR. Following the screening of the importance of

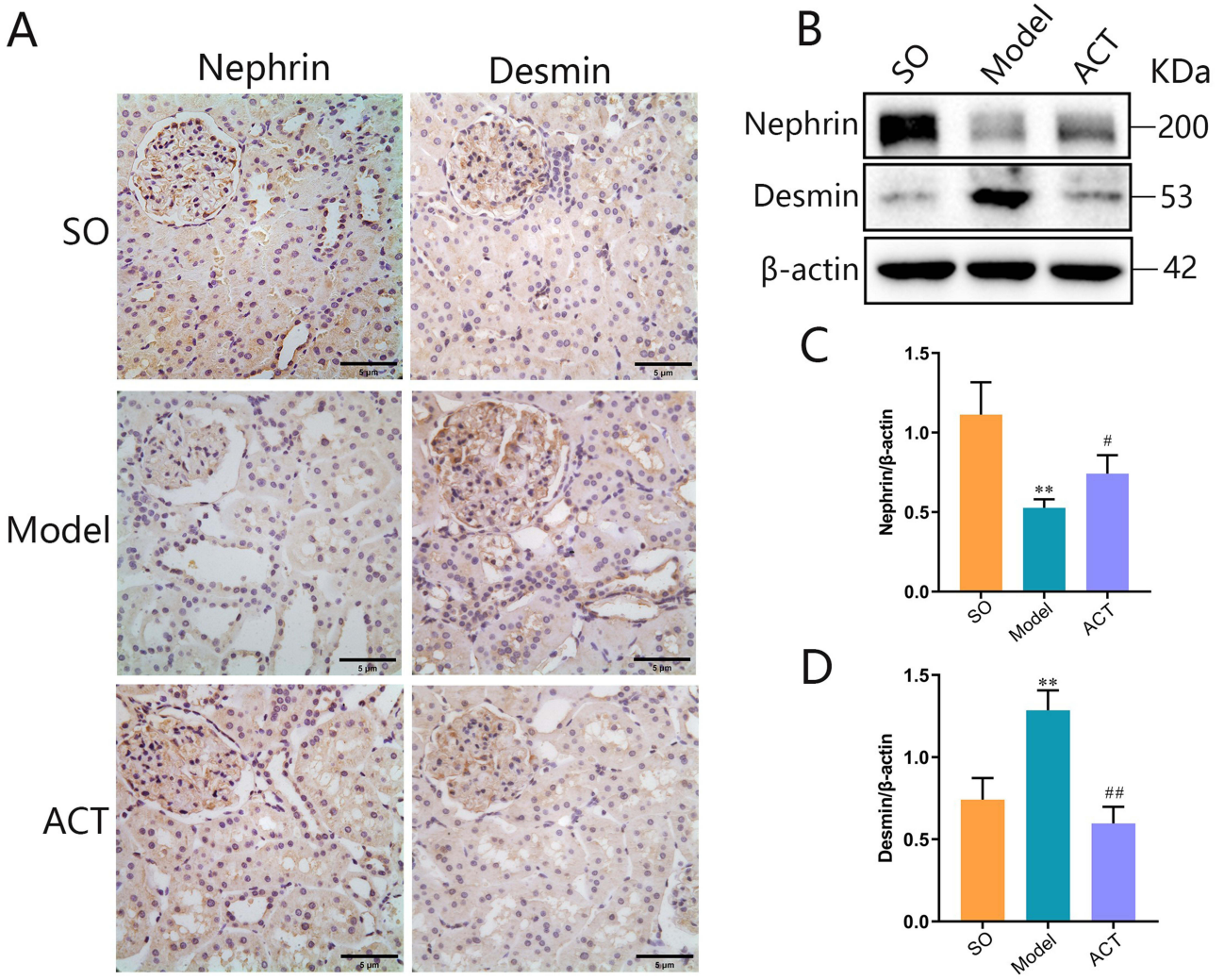

Figure 9 ACT attenuated podocyte injury in DKD rats. (**A**) Immunohistochemistry staining of nephrin and desmin (400× magnification). (**B**) Representative Western blots showing the detection of nephrin and desmin. (**C**) Relative protein expression of nephrin. (**C**) Relative protein expression of desmin. expression of desmin. Data are expressed as mean ± SD, n =5. **P<0.01 vs sham-operated (SO) group; #P<0.05 and ##P<0.01 vs model (Model) group.

individual targets within the pathway, we identified AKT1, AKT2, PIK3R1, PIK3CD, and NFκB1 as the core targets for DKD treatment through the PI3K/AKT pathway mediated by ACT.

The PI3K/AKT pathway is important to various biological processes including glucose homeostasis, lipid metabolism, protein synthesis, and cell proliferation.[23] PI3K, a family of intracellular lipid kinases, is categorized into three classes (I, II, III) predicated on their structural characteristics and substrate selectivity. Class I, the most extensively researched, is a heterodimer comprised of a regulatory subunit (P85) and a catalytic subunit (P110).[24] Furthermore, Class I is subdivided into IA and IB subunits based on molecular structural differences. The class IA consists of the regulatory subunits p85α, β, γ and the catalytic subunits p110α, β, δ, which are encoded by the genes PIK3R1, PIK3R2, PIK3R3 and PIK3CA, PIK3CB, PIK3CD respectively.[25] The p85 subunit engages in receptor binding, enzyme activation, and localization, whereas p110δ subunit is exclusive to leukocytes. Class I PI3Ks are activated by receptor tyrosine kinases (RTKs), catalyzing the phosphorylation of phosphatidylinositol 4,5-bisphosphate (PIP2) to generate phosphatidylinositol 3,4,5-trisphosphate (PIP3) on intracellular membranes. This synthesis facilitates the interaction between PIP3 and the PH domain of AKT, promoting the aggregation of AKT at the cell membrane and exposing its Thr308 phosphorylation site. Subsequently, the Thr308 site is phosphorylated by phosphoinositide-dependent protein kinase-1 (PDK1), activating AKT and influencing a range of downstream cellular and physiological processes. AKT is categorized into three isoforms

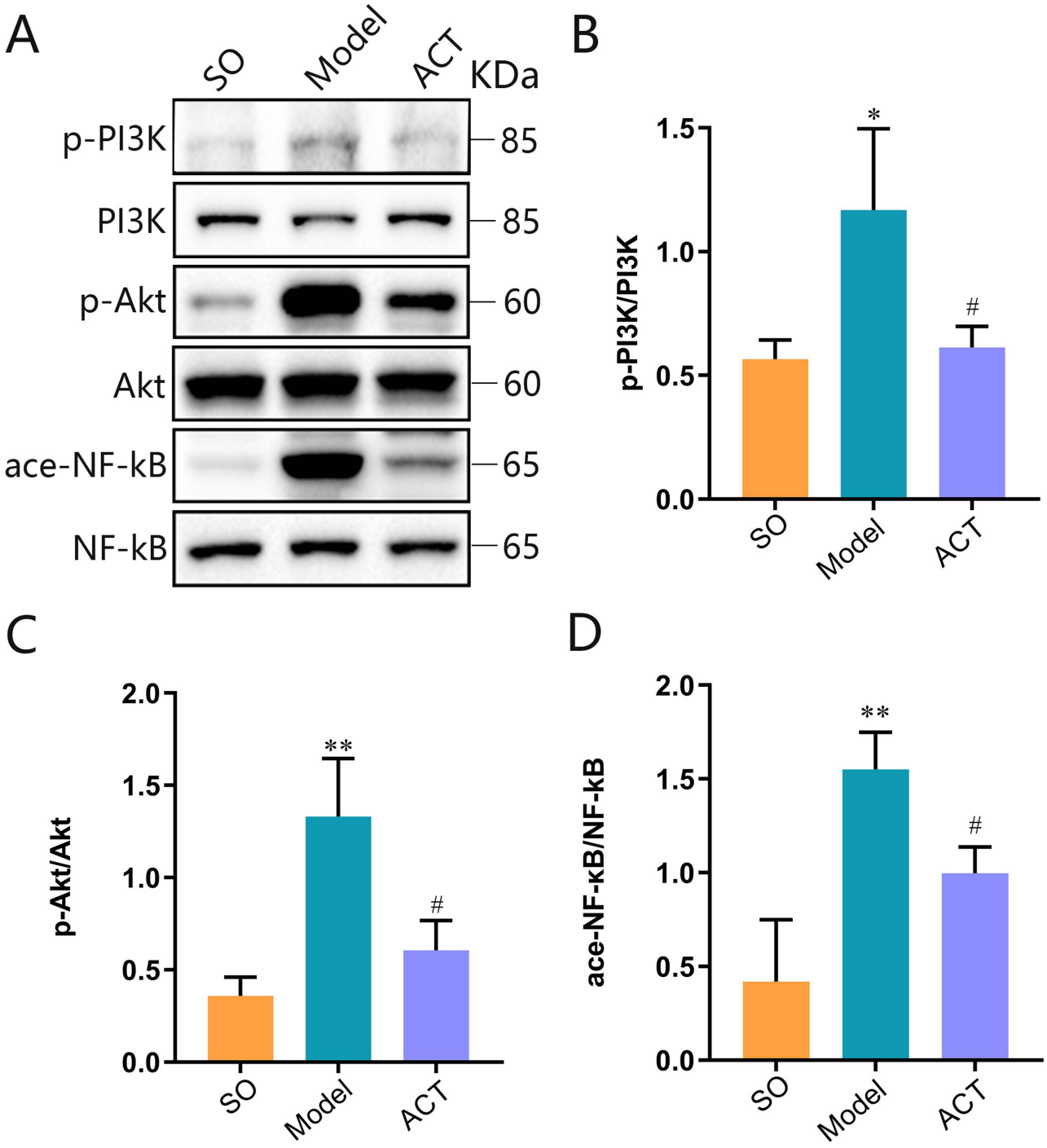

Figure 10 Validation of the predicted target proteins with Western blotting. (**A**) Representative Western blots showing the detection of p-PI3K, PI3K, p-Akt, Akt, ace-NF-κB and NF-κB. (**B-D**) The phosphorylation levels of AKT, PI3K and the acetylation of NF-κB decreased after treatment of ACT. Data are expressed as mean ± SD, n = 5. *P<0.05 and **P<0.01 vs sham-operated (SO) group; #P<0.05 vs model (Model) group.

(AKT1, AKT2 and AKT3) based on the variance in their serine/threonine residues. While AKT1 is ubiquitously expressed, AKT2 is primarily found in skeletal muscles and the liver, and AKT3 is predominantly expressed in the brain and testes.[26,27]

Therefore, we selected the core targets of the PI3K/AKT signaling pathway, PIK3R1, AKT1, and NF-κB1, to perform molecular docking with ACT. The favorable binding affinities observed support the hypothesis that ACT can exert nephroprotective effects in DKD through the PI3K/AKT/NF-κB pathway. Research has established that the PI3K/AKT

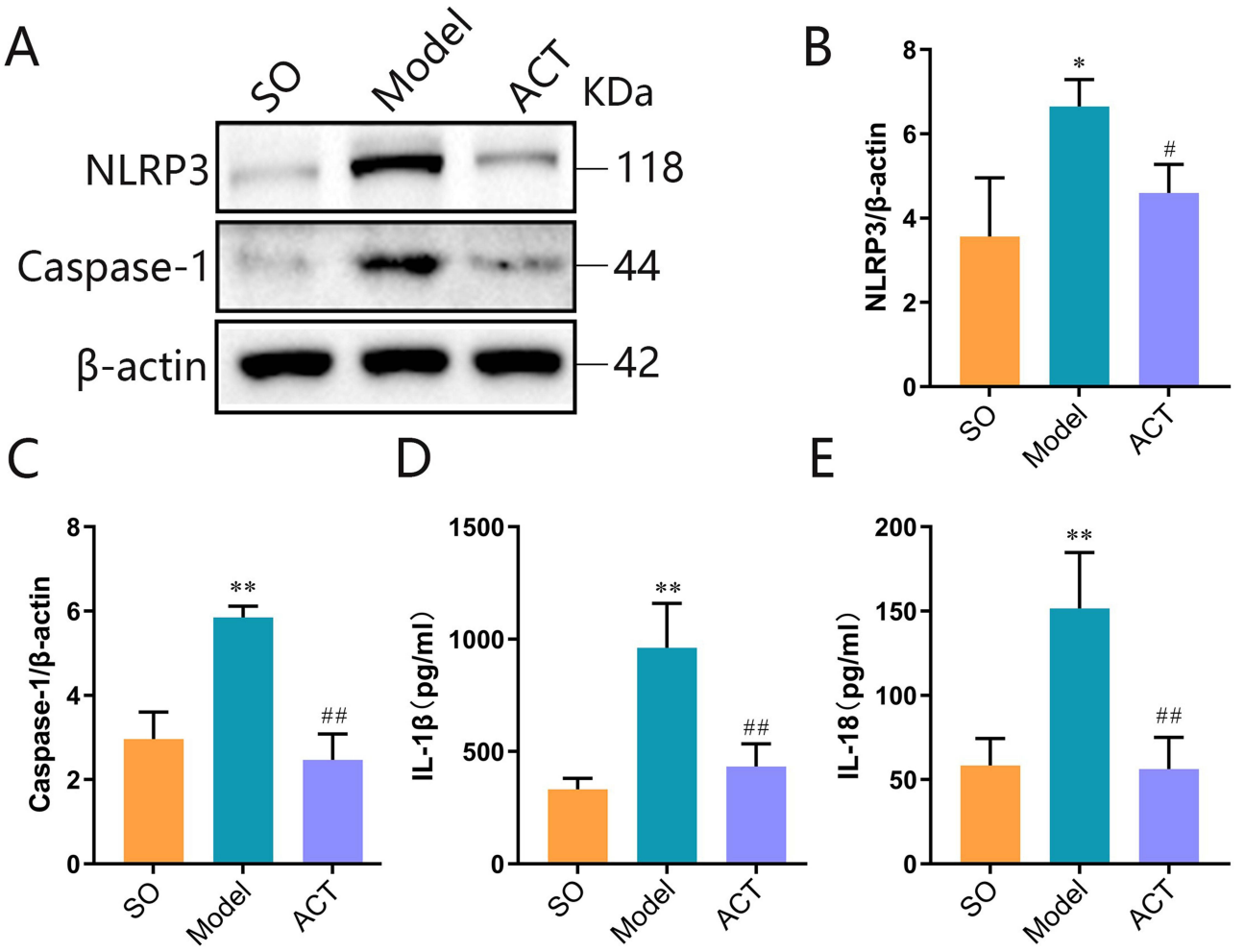

Figure 11 ACT attenuates renal pyroptosis levels. (**A**) Representative Western blot images displaying the detection of NLRP3 and Caspase-1. (**B-C**) Following treatment with ACT, levels of NLRP3 and Caspase-1 were both reduced. (**D-E**) ELISA analysis indicated that the expression levels of IL-1β and IL-18 both decreased following ACT treatment. Data are expressed as mean ± SD, n = 5. *P<0.05 and **P<0.01 vs sham-operated (SO) group; #P<0.05 and ##P<0.01 vs model (Model) group.

pathway is involved in diabetic nephropathy, mediating critical processes such as extracellular matrix accumulation, podocyte apoptosis, glomerular hypertrophy, mesangial cell proliferation and epithelial-mesenchymal transition (EMT).[28–30] Blockade of this pathway has demonstrated efficacy in mitigating the progression of DKD through mechanisms including activating autophagy, inhibiting oxidative stress, anti-inflammation, alleviating fibrosis and reducing apoptosis.[31–33] NF-κB, a crucial downstream component of the PI3K/AKT pathway, influences DKD pathogenesis in glomerular mesangial cells, endothelial cells, and podocytes by facilitating oxidative stress, augmenting inflammatory reactions, and initiating pyroptosis.[34,35] Pyroptosis, characterized as a pro-inflammatory programmed cell death, compounds renal dysfunction and intensifies renal fibrosis, highlighting its significance in DKD pathophysiology.[36] NF-κB is essential to pyroptotic mediation, catalyzing NLRP3 protein oligomerization and subsequent inflammasome assembly, and subsequently activating Caspase1. Caspase1 mediates the cleavage of the Gasdermin D (GSDMD) protein, forming pores on the cellular membrane. This cascade concurrently liberates a multitude of inflammatory cytokines, notably IL-1β and IL-18, driving both inflammation and pyroptosis.[37] Targeting pyroptosis emerges as a promising therapeutic strategy for DKD management.

In this study, we investigated the aforementioned pathway in vivo. Our results indicate that the PI3K/AKT and NF-κB expression levels were markedly elevated in the model group. Furthermore, we observed that ACT could modulates this signaling pathway, thereby inhibiting pyroptosis.

In conclusion, the findings suggest that ACT exerts its therapeutic effects on DKD by regulating the PI3K/AKT/NF-κB pathway, leading to a reduction in pyroptosis levels. However, the present study has several limitations. Firstly, not all the multi-pathway regulatory mechanisms of ACT on DKD were explored in this study. Furthermore, we did not employ MPC5 cells for in vitro experiments to directly demonstrate the protective effect of ACT on podocytes.

Conclusions

In this study, we investigated the pharmacological mechanism of ACT in treating DKD by network pharmacological analysis, molecular docking and experimental verification. Our findings indicate that ACT attenuates pyroptosis by modulating the PI3K/AKT/NF-κB signaling pathway, thereby exerting nephroprotective and therapeutic benefits for DKD. This research offers new insights into the exploration of the mechanism of TCM in DKD intervention and inspires advancements in new drug development.

Abbreviations

DKD, diabetic kidney disease; ACT, acteoside; PPI, utilizing protein-protein interaction; RAAS, renin-angiotensin-aldosterone system; ESRD, end-stage renal disease; CKD, chronic kidney disease; GO, gene ontology; BP, biological process; CC, cellular composition; MF, molecular function; KEGG, Kyoto Encyclopedia of Genes and Genomes; SO, sham operation; STZ, Streptozocin; BUN, blood urea nitrogen; Scr, serum creatinine; HE, Hematoxylin and Eosin; PAS, Periodic acid-Schiff; PASM, Periodic Acid-Silver Methenamine; DAB, 3,3'-Diaminobenzidine; PI3K, Phosphoinositide 3-kinase; AKT, Protein Kinase B; NF-KB, Nuclear Factor kappa-B; NLRP3, NOD-, LRR- and pyrin domain-containing protein 3; IL-1β, Interleukin-1 beta; IL-18, Interleukin-18; GFB, glomerular filtration barrier; FPs, foot processes; SD, slit diaphragm; GBM, glomerular basement membrane; RTK, receptor tyrosine kinase; EMT, epithelial-mesenchymal transition; GSDMD, Gasdermin D.

Author Contributions

All authors made a significant contribution to the work reported, whether that is in the conception, study design, execution, acquisition of data, analysis and interpretation, or in all these areas; took part in drafting, revising or critically reviewing the article; gave final approval of the version to be published; have agreed on the journal to which the article has been submitted; and agree to be accountable for all aspects of the work.

Funding

This study was supported by the National Natural Science Foundation of China (Grant Nos. 82374382, 81874443, 82074361, 82274293), school-level major project of Beijing University of Traditional Chinese Medicine (2023-JYB-JBZD-037), hospital-level project of Dongzhimen Hospital, Beijing University of Chinese Medicine (DZMG-XZYY-23002), Chinese Society of Traditional Chinese Medicine Practical Project (ZSL-003-02).

Disclosure

The authors declared that they have no conflicts of interest in this work.

References

1. Tuttle KR, Agarwal R, Alpers CE, et al. Molecular mechanisms and therapeutic targets for diabetic kidney disease. *Kidney Int*. 2022;102(2):248–260. doi:10.1016/j.kint.2022.05.012
2. Persson F, Rossing P. Diagnosis of diabetic kidney disease: state of the art and future perspective. *Kidney Int*. 2018;8(1):2–7. doi:10.1016/j.kisu.2017.10.003
3. Selby NM, Taal MW. An updated overview of diabetic nephropathy: diagnosis, prognosis, treatment goals and latest guidelines. *Diabetes Obes Metab*. 2020;22(1):3–15. doi:10.1111/dom.14007
4. Samsu N, Bellini MI. Diabetic nephropathy: challenges in pathogenesis, diagnosis, and treatment. *Biomed Res Int*. 2021;2021:1497449. doi:10.1155/2021/1497449
5. Valencia WM, Florez H. How to prevent the microvascular complications of type 2 diabetes beyond glucose control. *Bmj*. 2017;356:i6505. doi:10.1136/bmj.i6505

6. Yang C, Wang H, Zhao X, et al. CKD in China: evolving spectrum and public health implications. *Am J Kidney Dis*. 2020;76(2):258–264. doi:10.1053/j.ajkd.2019.05.032
7. Lu Z, Zhong Y, Liu W, Xiang L, Deng Y. The efficacy and mechanism of Chinese herbal medicine on diabetic kidney disease. *J Diabetes Res*. 2019;2019:2697672. doi:10.1155/2019/2697672
8. Lachowicz-Wiśniewska S, Pratap-Singh A, Kapusta I, et al. Flowers and leaves extracts of Stachys palustris l. exhibit stronger anti-proliferative, antioxidant, anti-diabetic, and anti-obesity potencies than stems and roots due to more phenolic compounds as revealed by UPLC-PDA-ESI-TQD-MS/MS. *Pharmaceuticals*. 2022;15(7):785. doi:10.3390/ph15070785
9. Wang Z, Xia Q, Liu X, et al. Phytochemistry, pharmacology, quality control and future research of Forsythia suspensa (Thunb.) Vahl: a review. *J Ethnopharmacol*. 2018;210:318–339. doi:10.1016/j.jep.2017.08.040
10. Zhao M, Qian D, Liu P, et al. Comparative pharmacokinetics of catalpol and acteoside in normal and chronic kidney disease rats after oral administration of rehmannia glutinosa extract. *Biomed Chromatogr*. 2015;29(12):1842–1848. doi:10.1002/bmc.3505
11. Chen X, Ge HZ, Lei SS, et al. Dendrobium officinalis six nostrum ameliorates urate under-excretion and protects renal dysfunction in lipid emulsion-induced hyperuricemic rats. *Biomed Pharmacother*. 2020;132:110765. doi:10.1016/j.biopha.2020.110765
12. Khan RA, Hossain R, Roy P, et al. Anticancer effects of acteoside: mechanistic insights and therapeutic status. *Eur J Pharmacol*. 2022;916:174699. doi:10.1016/j.ejphar.2021.174699
13. Khullar M, Sharma A, Wani A, et al. Acteoside ameliorates inflammatory responses through NFkB pathway in alcohol induced hepatic damage. *Int Immunopharmacol Apr*. 2019;69:109–117. doi:10.1016/j.intimp.2019.01.020
14. Lau CW, Chen ZY, Wong CM, et al. Attenuated endothelium-mediated relaxation by acteoside in rat aorta: role of endothelial [Ca2+]i and nitric oxide/cyclic GMP pathway. *Life Sci*. 2004;75(10):1149–1157. doi:10.1016/j.lfs.2003.12.031
15. Sheng GQ, Zhang JR, Pu XP, Ma J, Li CL. Protective effect of verbascoside on 1-methyl-4-phenylpyridinium ion-induced neurotoxicity in PC12 cells. *Eur J Pharmacol*. 2002;451(2):119–124. doi:10.1016/j.biopha.2020.110765
16. Gao W, Zhou Y, Li C, et al. Studies on the metabolism and mechanism of acteoside in treating chronic glomerulonephritis. *J Ethnopharmacol*. 2023;302(Pt A):115866. doi:10.1016/j.jep.2022.115866
17. Wang Q, Dai X, Xiang X, et al. A natural product of acteoside ameliorate kidney injury in diabetes db/db mice and HK-2 cells via regulating NADPH/oxidase-TGF-β/Smad signaling pathway. *Phytother Res*. 2021;35(9):5227–5240. doi:10.1002/ptr.7196
18. Li S, Zhang B. Traditional Chinese medicine network pharmacology: theory, methodology and application. *Chin J Nat Med*. 2013;11(2):110–120. doi:10.3724/SP.J.1009.2013.00110
19. Barlow DJ, Buriani A, Ehrman T, Bosisio E, Eberini I, Hylands PJ. In-silico studies in Chinese herbal medicines' research: evaluation of in-silico methodologies and phytochemical data sources, and a review of research to date. *J Ethnopharmacol*. 2012;140(3):526–534. doi:10.1016/j.jep.2012.01.041
20. Gao W, Gao S, Zhang Y, et al. Altered metabolic profiles and targets relevant to the protective effect of acteoside on diabetic nephropathy in db/db mice based on metabolomics and network pharmacology studies. *J Ethnopharmacol*. 2024;318(Pt B):117073. doi:10.1016/j.jep.2023.117073
21. Xiao Y, Ren Q, Wu L. The pharmacokinetic property and pharmacological activity of acteoside: a review. *Biomed Pharmacother*. 2022;153:113296. doi:10.1016/j.biopha.2022.113296
22. Barutta F, Bellini S, Gruden G. Mechanisms of podocyte injury and implications for diabetic nephropathy. *Clin Sci*. 2022;136(7):493–520. doi:10.1042/cs20210625
23. Abeyrathna P, Su Y. The critical role of Akt in cardiovascular function. *Vascul Pharmacol*. 2015;74:38–48. doi:10.1016/j.vph.2015.05.008
24. Long HZ, Cheng Y, Zhou ZW, Luo HY, Wen DD, Gao LC. PI3K/AKT signal pathway: a target of natural products in the prevention and treatment of alzheimer's disease and parkinson's disease. *Front Pharmacol*. 2021;12:648636. doi:10.3389/fphar.2021.648636
25. Xie Y, Shi X, Sheng K, et al. PI3K/Akt signaling transduction pathway, erythropoiesis and glycolysis in hypoxia (review). *Mol Med Rep*. 2019;19(2):783–791. doi:10.3892/mmr.2018.9713
26. Huang X, Liu G, Guo J, Su Z. The PI3K/AKT pathway in obesity and type 2 diabetes. *Int J Biol Sci*. 2018;14(11):1483–1496. doi:10.7150/ijbs.27173
27. Xu W, Yang Z, Lu N. A new role for the PI3K/Akt signaling pathway in the epithelial-mesenchymal transition. *Cell Adh Migr*. 2015;9(4):317–324. doi:10.1080/19336918.2015.1016686
28. Zhang X, Liang D, Chi ZH, et al. Effect of zinc on high glucose-induced epithelial-to-mesenchymal transition in renal tubular epithelial cells. *Int J Mol Med*. 2015;35(6):1747–1754. doi:10.3892/ijmm.2015.2170
29. Zhang Y, Wang Y, Luo M, et al. Elabela protects against podocyte injury in mice with streptozocin-induced diabetes by associating with the PI3K/Akt/mTOR pathway. *Peptides*. 2019;114:29–37. doi:10.1016/j.peptides.2019.04.005
30. Li Y, Zhao M, He D, et al. HDL in diabetic nephropathy has less effect in endothelial repairing than diabetes without complications. *Lipids Health Dis*. 2016;15:76. doi:10.1186/s12944-016-0246-z
31. Gao C, Fei X, Wang M, Chen Q, Zhao N. Cardamomin protects from diabetes-induced kidney damage through modulating PI3K/AKT and JAK/STAT signaling pathways in rats. *Int Immunopharmacol*. 2022;107:108610. doi:10.1016/j.intimp.2022.108610
32. Liu H, Chen W, Lu P, Ma Y, Liang X, Liu Y. Ginsenoside Rg1 attenuates the inflammation and oxidative stress induced by diabetic nephropathy through regulating the PI3K/AKT/FOXO3 pathway. *Ann Transl Med*. 2021;9(24):1789. doi:10.21037/atm-21-6234
33. Yang F, Qu Q, Zhao C, et al. Paecilomyces cicadae-fermented radix astragali activates podocyte autophagy by attenuating PI3K/AKT/mTOR pathways to protect against diabetic nephropathy in mice. *Biomed Pharmacother*. 2020;129:110479. doi:10.1016/j.biopha.2020.110479
34. Ke G, Chen X, Liao R, et al. Receptor activator of NF-κB mediates podocyte injury in diabetic nephropathy. *Kidney Int*. 2021;100(2):377–390. doi:10.1016/j.kint.2021.04.036
35. Ma Z, Liu Y, Li C, Zhang Y, Lin N. Repurposing a clinically approved prescription Colquhounia root tablet to treat diabetic kidney disease via suppressing PI3K/AKT/NF-kB activation. *Chin Med*. 2022;17(1):2. doi:10.1186/s13020-021-00563-7
36. Wang Y, Jin M, Cheng CK, Li Q. Tubular injury in diabetic kidney disease: molecular mechanisms and potential therapeutic perspectives. *Front Endocrinol*. 2023;14:1238927. doi:10.3389/fendo.2023.1238927
37. Williams BM, Cliff CL, Lee K, Squires PE, Hills CE. The role of the nlrp3 inflammasome in mediating glomerular and tubular injury in diabetic nephropathy. *Front Physiol*. 2022;13:907504. doi:10.3389/fphys.2022.907504